Jurnal Kejuruteraan 38(1) 2026: 301-309
https://doi.org/10.17576/jkukm-2026-38(1)-27

Kinetics and Kinetics-free Simulation of Oil Palm Biomass Waste Torrefaction

Yong Yung Sheng, Ruwaida Abdul Rasid* & Mazni Ismail

Faculty of Chemical and Process Engineering Technology,
Universiti Malaysia Pahang al-Sultan Abdullah, 26300 Pahang, Malaysia.

**Corresponding author: ruwaida@umpsa.edu.my*

Received 21 January 2025, Received in revised form 1 September 2025
Accepted 1 October 2025, Available online 30 January 2026

ABSTRACT

Torrefaction is a thermochemical process in which oil palm waste is heated to generate high calorific value, energy density, and a storable green fuel. This work aims to generate a computational model that can simulate the torrefaction process for the empty fruit bunch (EFB) and evaluate the model outcomes with and without the reaction kinetics. It is shown that the solid carbon mass fraction reduced steadily against temperature, while other liquids and gases increased as more volatile matter was released due to the decomposition of hemicellulose in the biomass. The heat duty decreased when the reactor's temperature increased, which is due to the decreased activation energy required for the decomposition reaction, as the increase of extractives, including the condensable and non-condensable products, acted as the catalyst for the decomposition to occur. The kinetic involvement in the model is proven to increase the accuracy of the product distribution as it has a higher similarity of the trend of distribution towards the literature compared to non-kinetics, specifically 86.41%, 76.05% and 89.23% error reduction for solids, liquids and gases, respectively. The heat duty of the kinetic model is more realistic due to the involvement of kinetic parameters in the study. In conclusion, applying computational and kinetic modelling can simulate the torrefaction process and will be further introduced to the industry.

Keywords: Oil palm waste; torrefaction; process simulation; kinetics; Aspen Plus

INTRODUCTION

The once dominant source of energy, fossil fuel, which makes up 80% of the world's supply, has diminished over the years (Moriarty & Honnery 2022). This has caused the shift of energy systems towards the usage of renewable energy sources, including not only solar, hydro and wind but also biomass that can contribute to the energy system in the generation of electricity for all usages (Castells et al. 2021). Biomass that can be obtained from agriculture, forestry, sludge, and other sources contributes to the effort of decreasing the carbon footprint and carbon dioxide release during the combustion process (Yang et al. 2023b). Therefore, the usage of lignocellulosic biomass in combustion, liquid biofuel production and combustible gases invites abundant advantages (Ajorloo et al. 2022; K N et al. 2022).

On the other hand, the application of biomass into industrial production has yet to be increased due to the high moisture content, low energy density and poor grindability (Kota et al. 2022). Therefore, pre-treating biomass with a thermochemical method named torrefaction is of utmost importance as it can remove the excess moisture content and volatile matter in the raw biomass, leaving the energy-dense, hydrophobic, high grindability and calorific value solid biofuel that can greatly improve the efficiency of the following reactions, such as combustion and gasification (Galbe & Wallberg 2019; Kongto et al. 2021).

Malaysia, as the second largest oil palm plantation country, generates tonnes of oil palm waste, and sadly, 90% of the waste has not been utilised fully in energy generation (Sellappah et al. 2016). Consequently, researchers have investigated oil palm wastes' torrefaction over the years, like the thermal degradation, functional groups and species of the volatiles released during the process (Chang et al. 2022), torrefaction influence on combustion kinetics (Castells et al. 2021), torrefaction in various atmospheres such as inert (Sulaiman, Uemura & Azizan 2016),

combustion flue gas (Uemura et al. 2017) and oxygen (Uemura et al. 2013, 2015) and mid-pressure torrefaction of empty fruit bunch (Hasan et al. 2022). While significant progress has been made in understanding the torrefaction process through experimental studies, there remains a critical gap in developing computational models that can accurately simulate the process on a scale. These studies often lack a comprehensive analysis of energy efficiency and process scalability, which are essential for industrial applications.

This is overcome through various empirical studies that have been conducted using computational software to develop the torrefaction simulation environment. These studies show that Aspen Plus can provide energy usage and efficiency data in a more time and money-effective manner. Studies were conducted on herb residue (Jiao et al. 2022), canola residue (Sarker et al. 2023), wheat straw, pine, grape pomace, manure, algae (Akbari, Oyedun & Kumar 2020) and poultry litter (Ayub et al. 2023) with the help of the stoichiometric reactors. It is a model that calculates the mass balance of the reaction based on the known stoichiometry of the reaction. The yield reactors, on the other hand, are useful when the kinetics and stoichiometry of the reaction are unknown. Studies were conducted on rice husk (Salisu, Gao & Quan 2021) and coal (Zheng et al. 2024). These models provide a simple method to obtain energy data, but cannot accurately estimate the product distribution without experimental data. On the contrary, kinetics-based reactors such as continuous stirred tank reactors and plug flow reactors depend on the kinetics of the reaction. They can estimate the outcome of the process at various temperatures and residence times. For birch (Bach, Skreiberg & Lee 2017b) and forest residue (Bach, Skreiberg & Lee 2017a), the researchers used a user-defined reactor with FORTRAN code linked with kinetics and found out that the drying process took up to 76-81% of the total heat of the overall process. A series of plug flow reactors based on Di Blasi and Lanzetta's two-step mechanism for wheat straw, where the attributes of the intermediate product were estimated using a correlation between the raw and final product of the torrefaction (Nikolopoulos et al. 2013). Kinetics data was also used in the torrefaction simulation using two yield-based reactors, simulating the two-step mechanism and volatile release using the anhydrous weight loss (AWL) model (Onsree, Jaroenkhasemmeesuk & Tippayawong 2020). This gives us an insight into the process, but the intermediate product is a modelled substance that is not realistic.

While efforts are being made to simulate the environment of the torrefaction reaction using the software, existing studies involving empty fruit bunch (EFB) focused on non-solid production processes, such as steam methane reforming (Sinaga, Napitupulu & Nur 2020) and biofuel production through fast pyrolysis (Janta-In, Wiriyalapsakul & Srinophakun 2022).These works often overlook the involvement of intermediate phases of the process and heat duty requirements that would be useful for energy optimisation. Performance differences evaluation between reactor types has not been systematically conducted. Therefore, a model of the torrefaction process is required to be developed so that the output distribution can be estimated, and the energy required for the process can be generated at a large scale.

This study aims to develop a comprehensive computational model using Aspen Plus to simulate the torrefaction process of oil palm biomass, specifically empty fruit bunches (EFB). The model seeks to compare the outcomes of simulations with and without the incorporation of reaction kinetics to evaluate their impact on product distribution, energy consumption, and process efficiency. By achieving this, the study intends to enhance the accuracy and applicability of torrefaction simulations for industrial-scale biomass utilisation, ultimately contributing to the optimisation of sustainable energy production from biomass.

METHODOLOGY

TORREFACTION PROCESS FLOW DIAGRAM

The overall process of the simulation was conducted using Aspen Plus v12.0, as illustrated in FIGURE 1, FIGURE 2 and FIGURE 3. A dryer was used to reduce the moisture content by 5% (wet basis) at 105 °C and 1 atm, followed by a torrefaction reactor (RYield, RGibbs, Rstoic and RCSTR) to show a comparison of non-kinetic and kinetic-based simulation at the temperatures of 250 °C, 275 °C and 300 °C at atmospheric pressure. A decomposition reactor at 25 °C and 1 atm was used before RCSTR and RGibbs, as biomass was identified as unconventional solids and could not be calculated in the reaction. The products of the process with more than 1 area% were depicted by other works of literature (Sukiran et al. 2021). The mild pyrolysis reactions from other literature were applied in the simulation of the kinetic reactor, as there is little information on the torrefaction process with kinetic parameters, with volatiles listed (Jaroenkhasemmeesuk et al. 2023). The kinetic reactor was based on a residence time of 30 minutes.

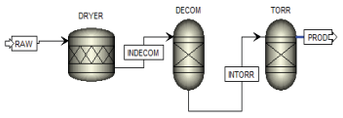

FIGURE 1. The Aspen Plus flowsheet for RGibbs.

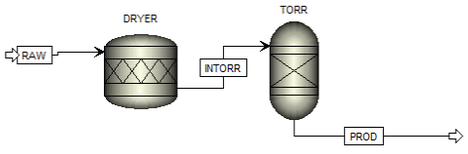

FIGURE 2. The flowsheet for RYield and RStoic.

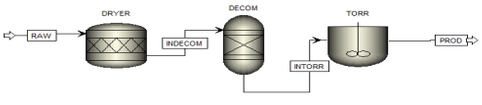

FIGURE 3. The flowsheet for RCSTR.

FEEDSTOCK PROPERTIES

Oil palm waste, which is EFB, was adopted from other work, as shown in TABLE 1 with a feed rate of 100 kg/hr. The proximate analysis consists of moisture content (MC), fixed carbon (FC), volatile matter (VM) and ash, whereas the sulfur-free ultimate analysis consists of carbon (C), hydrogen (H), nitrogen (N) and oxygen (O). As torrefaction is mainly due to the decomposition of hemicellulose and cellulose, the lignocellulose of EFB is assumed as hemicellulose and cellulose only (Yang et al. 2023a).

ASSUMPTIONS

The assumptions made in this work are as follows:

1. The stream class used was MIXNC, in which raw and torrefied biomass are considered non-conventional solids.
2. The Peng-Robinson-Boston-Mathias (PR-BM) properties method was used as it is the most commonly used method for hydrocarbon systems (Jiao et al. 2022).
3. A steady state was assumed for all calculations.
4. No pressure drops.
5. The ambient temperature is 25 °C.

TABLE 1. Physico-chemical properties of EFB used (Abdul Samad & Saleh 2022).

Properties	Values		
Temperature (°C)		Raw	250
Proximate Analysis (wt%)	MC	15.77	-
	FC	15.37	-
	VM	65.01	-
	Ash	3.85	-
Ultimate Analysis (wt%)	C	42.82	46.04
	H	6.07	6.16
	N	0.54	0.70
	O	50.57	47.10
Lignocellulosic properties (wt%)	Hemicellulose	42.47	-
	Cellulose	57.53	-

RESULTS AND DISCUSSION

NON-KINETIC MODELS

Several reactors in Aspen Plus were investigated to obtain the product yield of the torrefaction process for EFB, including RGibbs, RYield and RStoic.

RGIBBS

The RGibbs is a reactor model that applies the Gibbs energy of the system to zero, where single-phase chemical equilibrium is achieved (Jaroenkhasemmeesuk et al. 2023). The composition of the products of EFB estimated using the model is shown in FIGURE 4, where the components were depicted from the literature (Sukiran et al. 2021). It is noticeable that the solid carbon mass fraction reduced steadily against temperature, while other liquids and gases increased as more volatile matter was released due to the decomposition of hemicellulose in the biomass (Sukiran et al. 2021). The result of the heat duty of the RGibbs reactor is shown in TABLE 2. The heat duty decreased when the temperature of the reactor increased, which is due to the decreased activation energy required for the decomposition reaction to occur, as the increase in extractives acts as the catalyst for the decomposition to occur (Cardarelli, Pinzi & Barbanera 2022). However, when compared to literature, the product distribution is of huge difference, where the highest should be solid (50.91% error), followed by gases (59.40% error) and liquids (877.26% error) (Sukiran et al. 2021). The error should be less than 5% to show the accuracy of the model when compared to the literature (Yek et al. 2022). The error shows that RGibbs is unable to predict the product of the

torrefaction process accurately, as Gibbs's free energy minimisation method of the model depends on the fugacity of the real gases, but the high amount of liquid products available in the process would cause the calculation of the output to be inaccurate (Zhao et al. 2023).

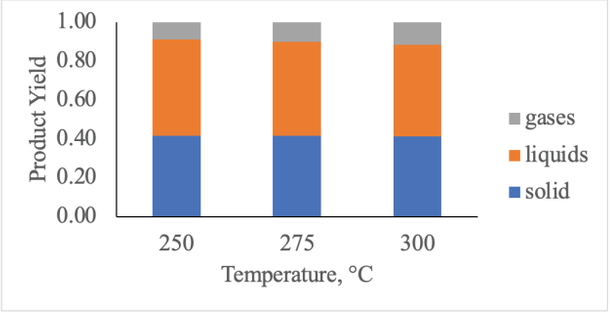

FIGURE 4. Mass distribution of the products at various temperatures of EFB using RGibbs.

TABLE 2. Heat duty of the Gibbs reactor across different temperatures of EFB.

Types of oil palm waste	EFB		
Temperature, °C	250	275	300
Heat duty, Btu/hr	513795.1	509033.6	503878.7

RYIELD

The yield reactor is a model that simulates the output of the reaction according to the product distribution from experimental works, and available components of the liquid and gases were normalised into mass yield (Sukiran et al. 2021). The result of the simulation compared to the yield of the literature normalised is as shown in TABLE 3 where the product with less than 1 area % was not considered. The results are acceptable with minimal error found. However, this is only limited to the result available from the literature, as RYield is not temperature dependent and is unable to predict the possible products of the reaction at different temperatures, since the yield of the output product is the specified parameter.

TABLE 3. Comparison of product mass yield of literature to current work at 250 °C.

Component	Experimental mass yield, wt. fraction (Sukiran et al. 2021)	Simulated mass yield, Wt. fraction (this study)	Error, %
Torrefied EFB	0.7800	0.7800	0.00
Carbon monoxide, CO	0.0461	0.0461	0.00
Carbon dioxide, CO_2	0.1382	0.1382	0.00
Methane, CH_4	0.0058	0.0058	0.01
Acetic acid, CH_3COOH	5.2096×10^{-3}	5.2100×10^{-3}	0.01
Propanoic acid, C_2H_5COOH	8.8787×10^{-4}	8.8800×10^{-4}	0.01
1-hydroxy-2-butanenone, $C_4H_8O_2$	1.1337×10^{-3}	1.1340×10^{-3}	0.03
1,2-cyclopentanedione, $C_5H_6O_2$	5.9738×10^{-4}	5.9700×10^{-4}	0.06
3-pentanone, $C_5H_{10}O$	2.3687×10^{-4}	2.3700×10^{-4}	0.06
Propanol, C_3H_7OH	5.7205×10^{-4}	5.7200×10^{-4}	0.01
1,2-benzenediol, $C_6H_6O_2$	8.2828×10^{-4}	8.2800×10^{-4}	0.03
Phenol, C_6H_6O	1.9426×10^{-4}	1.9430×10^{-3}	0.02
Phenol,2-methoxy, $C_7H_8O_2$	5.4822×10^{-4}	5.4800×10^{-4}	0.04
Phenol,3,4-dimethoxy, $C_8H_{10}O_3$	2.7709×10^{-4}	2.7700×10^{-4}	0.03
Furfural, $C_5H_4O_2$	1.5642×10^{-4}	1.5600×10^{-4}	0.27
Water, H_2O	0.0176	0.0176	0.00

RSTOIC

The stoichiometric reactor depends on the stoichiometry of the reaction to calculate the thermodynamic properties of the reaction (Jaroenkhasemmeesuk et al. 2023). However, for the case of torrefaction, the research conducted was heavily mass-dependent, where the theoretical mass balance was not taken into consideration. Therefore, Equation (1) has been created to investigate the stoichiometry coefficients α to ρ. An atomic balance was conducted using the product yield from literature, where it was not in balance (Sukiran et al. 2021). Therefore, backwards calculations were made to balance carbon, hydrogen, and oxygen atoms. The results of the calculations and the simulated results are shown in TABLE 4 (Sukiran et al. 2021). This can only be achieved by considering a factor of 0.0016 H_2 at the inlet and 0.0017833 O_2 at the outlet to achieve a balanced equation. It is worth noting that the error of the simulated results using the stoichiometry coefficient calculated is minimal, showing the accuracy of the model.

$$C_aH_bO_cN_d = \alpha\, C_eH_fO_gN_h + \begin{cases} \beta\, CO \\ \gamma\, CO_2 \\ \delta\, CH_4 \\ \varepsilon\, CH_3COOH \\ \zeta\, C_2H_5COOH \\ \eta\, C_4H_8O_2 \\ \theta\, C_5H_6O_2 \\ \iota\, C_5H_{10}O \\ \kappa\, C_3H_7OH \\ \lambda\, C_6H_6O_2 \\ \mu\, C_6H_6O \\ \nu\, C_7H_8O_2 \\ \xi\, C_8H_{10}O_3 \\ \pi\, C_5H_4O_2 \\ \rho\, H_2O \end{cases} \quad (1)$$

TABLE 4. Comparison of the simulated and experimental results of EFB at 250 °C (Sukiran et al. 2021)

Component	Experimental mass flow, kg/hr (Sukiran et al. 2021)	Stoichiometry coefficient	Simulated mass flow, kg/hr (this study)	Error, %
Torrefied EFB	74.4362	0.7521	73.6266	1.09
Carbon monoxide, CO	4.3956	1.6031×10^{-3}	4.3958	0.00
Carbon dioxide, CO_2	13.1868	3.0609×10^{-3}	13.1874	0.00
Methane, CH_4	0.5495	3.5065×10^{-4}	0.5507	0.23
Acetic acid, CH_3COOH	0.4972	8.4209×10^{-5}	0.4951	0.42
Propanoic acid, C_2H_5COOH	0.0847	1.1684×10^{-5}	0.0847	0.00
1-hydroxy-2-butanenone, $C_4H_8O_2$	0.1082	1.2543×10^{-3}	0.1082	0.00
1,2-cyclopentanedione, $C_5H_6O_2$	0.0570	5.9361×10^{-6}	0.0570	0.00
3-pentanone, $C_5H_{10}O$	0.0226	2.6808×10^{-6}	0.0226	0.00
Propanol, C_3H_7OH	0.0546	9.2795×10^{-6}	0.0546	0.00
1,2-benzenediol, $C_6H_6O_2$	0.0790	7.4010×10^{-6}	0.0798	0.93
Phenol, C_6H_6O	0.1854	2.0055×10^{-5}	0.1848	0.33
Phenol,2-methoxy, $C_7H_8O_2$	0.0523	4.3050×10^{-6}	0.0523	0.00
Phenol,3,4-dimethoxy, $C_8H_{10}O_3$	0.0264	1.7521×10^{-6}	0.0264	0.00
Furfural, $C_5H_4O_2$	0.0149	1.5870×10^{-6}	0.0149	0.00
Water, H_2O	1.6805	9.5106×10^{-4}	1.6773	0.19

KINETIC MODELS

In this study, RCSTR was used to represent the kinetic-based model.

RCSTR

The kinetic model represented by the RCSTR model block assembles a continuously stirred tank reactor that requires the input of kinetic parameters such as activation energy and pre-exponential factor. Table 5 shows the names of the components involved in the mild pyrolysis reactions, while Table 6 shows the reaction equations used in the work that were extracted from the literature. The results are shown in Table 7 (Jaroenkhasemmeesuk et al. 2023; Ranzi et al. 2014). When the temperature increases, the solid composition decreases as more volatile matter is released throughout the process. Moreover, the liquid composition is higher than the gas composition, similar to the work by Peter et al., where the liquids are more than the gases by 65 wt% for pine wood at 500 °C, but 16 wt% for EFB at 250 °C (Peters et al. 2017). However, this is in reverse compared to the torrefaction experimental work by Sukiran et al., where the gas composition is more than the liquid by 16 wt% (Sukiran et al. 2021), which is due to the application of pyrolytic kinetics that emphasise the conversion of the solid hemicellulose and cellulose to liquid products. The heat duty of the reactor increases with temperature as the increment of the heat available in the system enables the atoms of the volatile matter to break free from the solid biomass (Blanksby & Ellison 2003).

TABLE 5. The component names involved in Table 6.

Component ID	Type	Component Name
CELL	Solid	Cellulose
CELLA	Conventional	Activated Cellulose
HAA	Conventional	Haloacetic acids
HMFU	Conventional	Hydroxymethylfurfural
LVG	Conventional	Vinylglycine
HCE	Solid	Hemicellulose

TABLE 6. Reaction equation of pyrolysis (Jaroenkhasemmeesuk et al. 2023; Ranzi et al. 2014).

Reactions	Rate	Units
$CELL \rightarrow CELLA$	$k = 8 \times 10^{13} \exp(-46000/RT)$	[s^{-1}]
$CELLA \rightarrow 0.95\ HAA + 0.25\ Glyoxal + 0.20\ CH_3CHO + 0.20\ C_3H_6O + 0.25\ HMFU + 0.20\ CO_2 + 0.15\ CO + 0.90\ H_2O + 0.65\ Char$	$k = 1 \times 10^{19} \exp(-30000/RT)$	[s^{-1}]
$CELLA \rightarrow LVG$	$k = 4T \exp(-10000/RT)$	[s^{-1}]
$CELL \rightarrow 5\ H_2O + 6\ Char$	$k = 8 \times 10^{7} \exp(-32000/RT)$	[s^{-1}]
$HCE \rightarrow 0.4\ HCE1 + 0.6\ HCE2$	$k = 1 \times 10^{10} \exp(-31000/RT)$	[s^{-1}]
$HCE1 \rightarrow 2.5\ H_2 + 0.125\ H_2O + CO + CO_2 + 0.5\ CH_2O + 0.25\ CH_3OH + 0.125\ C_2H_5OH + 2\ Char$	$k = 3 \times 10^{9} \exp(-27000/RT)$	[s^{-1}]
$HCE1 \rightarrow XYLOSE$	$k = 3T \exp(-11000/RT)$	[s^{-1}]
$HCE2 \rightarrow 1.5\ H_2 + 0.125\ H_2O + 0.2\ CO_2 + 0.7\ CH_2O + 0.25\ CH_3OH + 0.125\ C_2H_5OH + 0.8\ G\{COH_2\} + 2\ Char$	$k = 1 \times 10^{10} \exp(-33000/RT)$	[s^{-1}]

TABLE 7. The product yield of pyrolysis kinetics and the heat duty of the reactor of EFB at various temperatures.

Temperature, °C	250	275	300
Components wt. fraction			
Solid	0.8340	0.7278	0.6142
Liquid	0.1630	0.2692	0.3828
Gas	0.0017	0.0019	0.0021
Heat duty, Btu/hr	21770.6	39785.3	58076.4

COMPARISON OF THE KINETICS AND NON-KINETICS MODEL PREDICTIONS.

Figure 5 shows the comparison of product distribution of the non-kinetic model, specifically the Gibbs reactor and the kinetic model, CSTR. The distribution of solids in CSTR is higher than that in the Gibbs reactor, while the amount of liquid and gaseous products simulated by the Gibbs reactor is higher, showing that the application of kinetics will enhance the production of solids, which is closer to experimental work (Sukiran et al. 2021). As shown in TABLE 2 and Table 7, there is a huge difference in the heat duty that the RGibbs generates higher heat duty compared to RCSTR. This is due to the RCSTR can calculate the heat duty required using the activation energy, temperature and exergy loss provided, which gives a more accurate amount compared to RGibbs, which calculates the heat duty using the standard enthalpy of formation of the reactants and products (Demirel 2008). The amount of volatiles generated from the kinetics reaction is less compared to the non-kinetics model, where more energy is used even under the same temperature. At the same time, RGibbs operates and runs the calculations until the process reaches equilibrium, which would overestimate the energy required to maintain the temperature of the reactor and not always represent the actual process conditions (Chen et al. 2012). The gaseous volatiles are less than the liquid volatiles in RCSTR is due to the specification that the model focuses more on the solid and liquid phases, where low temperature tends to favour liquid yields compared to gases (Miranda, Filho & Maciel 2019). The kinetic involvement in the model is proven to increase the accuracy of the product distribution as it has a higher similarity of the trend of distribution towards the literature compared to non-kinetics, specifically 86.41%, 76.05% and 89.23% error reduction for solids, liquids and gases, respectively.

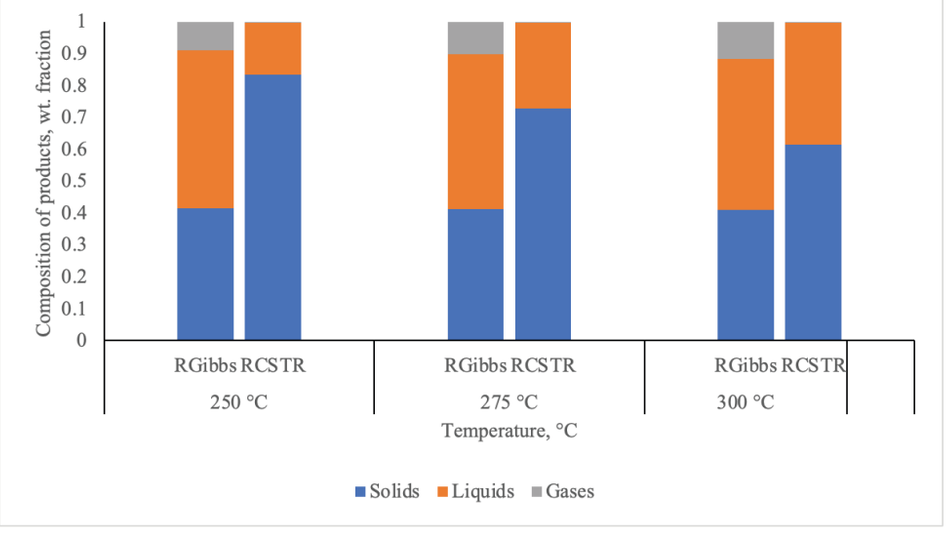

FIGURE 5. Comparison of the product distribution of non-kinetics to the kinetics model

CONCLUSION

In this study, a complete torrefaction model was built in Aspen Plus v12.0 software. For non-kinetic approaches, they provide easy solutions when essential information is not available, with respective pros and cons. In this study, stoichiometry coefficient has been calculated and proven using RStoic, which would help in the scale-up of the process, but is limited to a particular temperature. The accuracy of RGibbs in estimating heat duty and product distribution is way lower compared to experimental data due to the presence of three phases and non-conventional solid biomass, increasing the challenge of not overestimating the heat duty. RYield was unable to estimate the product distribution between the temperature. The application of kinetic data in RCSTR has proven to increase the accuracy and reduce the error % of product distribution. Future recommendations would include extensive interpolation of product distribution between temperature and compare with Aspen Plus, expand the application of kinetics to other types of biomass like mesocarp fibre and palm kernel shell, and include lignin pyrolysis kinetics data in RCSTR for biomass with higher lignin composition.

ACKNOWLEDGEMENT

The authors would like to acknowledge the support of the Faculty of Chemical and Process Engineering and Universiti Malaysia Pahang al-Sultan Abdullah for financial support through the Doctoral Research Scheme (DRS) and research grants (PGRS220363, RDU243307).

DECLARATION OF COMPETING INTEREST

None.

REFERENCES

Abdul Samad, N.A.F. & Saleh, S. 2022. Analysis of volatile composition released from torrefaction of empty fruit bunch. *Materials Today: Proceedings* 57: 1202–1207.

Ajorloo, M., Ghodrat, M., Scott, J. & Strezov, V. 2022. Recent advances in thermodynamic analysis of biomass gasification: A review on numerical modelling and simulation. *Journal of the Energy Institute* 102: 395–419.

Akbari, M., Oyedun, A.O. & Kumar, A. 2020. Techno-economic assessment of wet and dry torrefaction of biomass feedstock. *Energy* 207: 118287.

Ayub, Y., Zhou, J., Ren, J. & He, C. 2023. An innovative integration of torrefaction, gasification, and solid oxide fuel cell for carbon–neutral utilization of biomass waste: Process development, economic, exergy, advanced exergy, and exergoeconomics analysis. *Energy Conversion and Management* 292: 117426.

Bach, Q.-V., Skreiberg, Ø. & Lee, C.-J. 2017a. Process modeling and optimization for torrefaction of forest residues. *Energy* 138: 348–354.

Bach, Q.-V., Skreiberg, Ø. & Lee, C.-J. 2017b. Process modeling for torrefaction of birch branches. *Energy Procedia* 142: 395–400.

Blanksby, S.J. & Ellison, G.B. 2003. Bond Dissociation Energies of Organic Molecules. *Accounts of Chemical Research* 36(4): 255–263.

Cardarelli, A., Pinzi, S. & Barbanera, M. 2022. Effect of torrefaction temperature on spent coffee grounds thermal behaviour and kinetics. *Renewable Energy* 185: 704–716.

Castells, B., Amez, I., Medic, L. & García-Torrent, J. 2021. Torrefaction influence on combustion kinetics of Malaysian oil palm wastes. *Fuel Processing Technology* 218: 106843.

Chang, S.S., Sambeth, S.K., Abdul Samad, N.A.F. & Saleh, S. 2022. Effect of torrefaction on thermal degradation and functional group of oil palm solid waste. *Materials Today: Proceedings* 57: 1248–1255.

Chen, S.-H., Cao, Z.-K., Shi, J., Jiang, Q.-Y. & Zhou, H. 2012. Steady-state simulation of fixed bed for coal gasification using ASPEN PLUS. *Meitan Xuebao/ Journal of the China Coal Society* 37(SUPPL. 1): 167–172.

Demirel, Y. 2008. Retrofit of distillation columns in a methanol plant. *AIChE Annual Meeting, Conference Proceedings*, hlm. .

Galbe, M. & Wallberg, O. 2019. Pretreatment for biorefineries: A review of common methods for efficient utilisation of lignocellulosic materials. *Biotechnology for Biofuels* 12(1).

Hasan, M.F., Omar, M.S., Sukiran, M.A., Nyakuma, B.B. & Muhamad Said, M.F. 2022. Torrefaction of fibrous empty fruit bunch under mild pressurization technique. *Renewable Energy* 194: 349–358.

Janta-In, C., Wiriyalapsakul, K. & Srinophakun, T.R. 2022. Environmental and economic analysis of a biodiesel power plant derived from the fast pyrolysis of empty fruit bunches. *Asia-Pacific Journal of Science and Technology* 27(2).

Jaroenkhasemmeesuk, C., Tippayawong, N., Shimpalee, S., Ingham, D.B. & Pourkashanian, M. 2023. Improved simulation of lignocellulosic biomass pyrolysis plant using chemical kinetics in Aspen Plus® and comparison with experiments. *Alexandria Engineering Journal* 63: 199–209.

Jiao, L., Li, J., Yan, B., Chen, G. & Ahmed, S. 2022. Microwave torrefaction integrated with gasification: Energy and exergy analyses based on Aspen Plus modeling. *Applied Energy* 319: 119255.

K N, Y., T, P.D., P, S., S, K., R, Y.K., Varjani, S., AdishKumar, S., Kumar, G. & J, R.B. 2022. Lignocellulosic biomass-based pyrolysis: A comprehensive review. *Chemosphere* 286: 131824.

Kongto, P., Palamanit, A., Chaiprapat, S. & Tippayawong, N. 2021. Enhancing the fuel properties of rubberwood biomass by moving bed torrefaction process for further applications. *Renewable Energy* 170: 703–713.

Kota, K.B., Shenbagaraj, S., Sharma, P.K., Sharma, A.K., Ghodke, P.K. & Chen, W.-H. 2022. Biomass torrefaction: An overview of process and technology assessment based on global readiness level. *Fuel* 324: 124663.

Miranda, N.T., Filho, R.M. & Maciel, M.R.W. 2019. Sugarcane bagasse fast pyrolysis simulation: A thermodynamic equilibrium approach. *Chemical Engineering Transactions* 74: 175–180.

Moriarty, P. & Honnery, D. 2022. Introduction to Global Energy Challenges BT - Switching Off: Meeting Our Energy Needs in A Constrained Future. Dlm. Moriarty, P. & Honnery, D. (pnyt.). hlm. 1–13. Springer Singapore: Singapore.

Nikolopoulos, N., Isemin, R., Atsonios, K., Kourkoumpas, D., Kuzmin, S., Mikhalev, A., Nikolopoulos, A., Agraniotis, M., Grammelis, P. & Kakaras, Em. 2013. Modeling of Wheat Straw Torrefaction as a Preliminary Tool for Process Design. *Waste and Biomass Valorization* 4(3): 409–420.

Onsree, T., Jaroenkhasemmeesuk, C. & Tippayawong, N. 2020. Techno-economic assessment of a biomass torrefaction plant for pelletized agro-residues with flue gas as a main heat source. *Energy Reports* 6: 92–96.

Peters, J.F., Banks, S.W., Bridgwater, A. V. & Dufour, J. 2017. A kinetic reaction model for biomass pyrolysis processes in Aspen Plus. *Applied Energy* 188: 595–603.

Ranzi, E., Corbetta, M., Manenti, F. & Pierucci, S. 2014. Kinetic modeling of the thermal degradation and combustion of biomass. *Chemical Engineering Science* 110: 2–12.

Salisu, J., Gao, N. & Quan, C. 2021. Techno-economic Assessment of Co-gasification of Rice Husk and Plastic Waste as an Off-grid Power Source for Small Scale Rice Milling - an Aspen Plus Model. *Journal of Analytical and Applied Pyrolysis* 158: 105157.

Sarker, T.R., German, C.S., Borugadda, V.B., Meda, V. & Dalai, A.K. 2023. Techno-economic analysis of torrefied fuel pellet production from agricultural residue via integrated torrefaction and pelletization process. *Heliyon* 9(6): e16359.

Sellappah, V., Uemura, Y., Hassan, S., Sulaiman, M.H. & Lam, M.K. 2016. Torrefaction of Empty Fruit Bunch in the Presence of Combustion Gas. *Procedia Engineering* 148: 750–757.

Sinaga, F.T.H., Napitupulu, F.H. & Nur, T.B. 2020. Hydrogen Gas Production Simulation Utilizing Empty Fruit Bunch of Oil Palm Pyrolysis Unit by Steam Methane Reforming Process. *Journal of Physics: Conference Series*, hlm. . Institute of Physics Publishing.:

Sukiran, M.A., Wan Daud, W.M.A., Abnisa, F., Nasrin, A.B., Abdul Aziz, A. & Loh, S.K. 2021. A comprehensive study on torrefaction of empty fruit bunches: Characterization of solid, liquid and gas products. *Energy* 230: 120877.

Sulaiman, M.H., Uemura, Y. & Azizan, M.T. 2016. Torrefaction of Empty Fruit Bunches in Inert Condition at Various Temperature and Time. *Procedia Engineering* 148: 573–579.

Uemura, Y., Omar, W., Othman, N.A., Yusup, S. & Tsutsui, T. 2013. Torrefaction of oil palm EFB in the presence of oxygen. *Fuel* 103: 156–160.

Uemura, Y., Saadon, S., Osman, N., Mansor, N. & Tanoue, K. 2015. Torrefaction of oil palm kernel shell in the presence of oxygen and carbon dioxide. *Fuel* 144: 171–179.

Uemura, Y., Sellappah, V., Trinh, T.H., Hassan, S. & Tanoue, K. 2017. Torrefaction of empty fruit bunches under biomass combustion gas atmosphere. *Bioresource Technology* 243: 107–117.

Yang, W., Yang, F., Zhang, X., Zhu, P., Peng, H., Chen, Z., Che, L., Zhu, S. & Wu, S. 2023a. Investigation of holocellulose-lignin interactions during pyrolysis of wood meal by TGA-FTIR. *Biomass Conversion and Biorefinery* 13(5): 3731–3740.

Yang, Y., Qu, X., Huang, G., Ren, S., Dong, L., Sun, T., Liu, P., Li, Y., Lei, T. & Cai, J. 2023b. Insight into lignocellulosic biomass torrefaction kinetics with case study of pinewood sawdust torrefaction. *Renewable Energy* 215: 118941.

Yek, P.N.Y., Kong, S.H., Law, M.C., Xia, C., Liew, R.K., Sie, T.S., Lim, J.W. & Lam, S.S. 2022. Microwave torrefaction of empty fruit bunch pellet: Simulation and validation of electric field and temperature distribution. *Journal of Bioresources and Bioproducts* 7(4): 270–277.

Zhao, Y., Yao, J., Chen, G., Liu, J., Cheng, Z., Wang, L., Yi, W. & Xu, S. 2023. Energy, efficiency, and environmental analysis of hydrogen generation via plasma co-gasification of biomass and plastics based on parameter simulation using Aspen plus. *Energy Conversion and Management* 295: 117623.

Zheng, J., Zhang, H., Gong, X. & Zhang, Y. 2024. The integration of biomass torrefaction with coal gasification: Performance study and process simulation. *Journal of Analytical and Applied Pyrolysis* 180: 106559.